PARTICLE FORMATION OF *Casearia sylvestris* EXTRACT USING A SUPERCRITICAL ANTI-SOLVENT PROCESS

P. BENELLI[1], S. R. ROSSO COMIM[1], R. C. PEDROSA[2], J. V. de OLIVEIRA[1], S. R. S. FERREIRA[1]

[1]Universidade Federal de Santa Catarina, Departamento de Engenharia Química e Engenharia de Alimentos
[2]Universidade Federal de Santa Catarina, Departamento de Bioquímica
E-mail para contato: patybenelli@gmail.com

ABSTRACT - This research aimed the encapsulation of guaçatonga (Casearia sylvestris) extract in the biopolymer Pluronic F127 by means of supercritical anti-solvent (SAS) technique. The system was composed by guaçatonga extract, Pluronic F127, organic solvent (ethanol or ethyl acetate) and supercritical carbon dioxide (CO_2). Supercritical C. sylvestris extract was obtained at 50oC, 300 bar and CO_2 flow rate of 8.3 ± 2 g/min added of 5% (wt/wt) of ethanol, for 3.5 h of extraction. SAS conditions applied for the encapsulation ranged from 110 to 170 bar at 35oC and 45oC, based on precipitation tests and on the phase behavior of the system. The morphology of the particles obtained by SAS method and the particle size were characterized by scanning electronic microscopy, being considered as shapeless within the micrometric range. The interaction between the polymer and the encapsulated extract was verified by differential scanning calorimetry indicating that co-precipitated particles were produced.

1. INTRODUCTION

Casearia sylvestris is a medicinal plant native from Brazil and popularly known as "guaçatonga" and "erva-de-bugre". In folk medicine its leaves are used for skin and oral wound healing and it is also applied as topical anesthetic and antiseptic and anti-ulceration agent (Ferreira et al., 2010; Esteves et al., 2011). Phytochemical investigations revealed that some compounds isolated from this plant present biological potential such as antitumor, cytotoxic, antifungal and anti-inflammatory activities (Oberlies et al., 2002; Oliveira et al., 2009; Santos et al., 2010).

Considering biological attributes, the interest of food and pharmaceutical industries in preserving these properties, by means of protective methods such as coating or encapsulating (inside a carrier agent such as biopolymer), is significantly rising (Reverchon et al., 2000; Jung et al., 2001). Several supercritical fluid-based techniques of micronization and encapsulation, employing mainly CO_2, have been proposed in order to obtain solid particles with better control in particle size, size distribution, morphology and crystalline structure, which are difficult to obtain using traditional methods (Reverchon et al., 2003; Franceschi et al., 2008; Michielin et al., 2009). The high pressure technology allows the production of particulated materials preserving the active compounds quality, which is difficult to achieve by traditional techniques due to the presence of organic solvent residues and relatively high

45 processing temperatures (Miguel et al., 2008; Varona et al., 2010). Supercritical anti-solvent
46 (SAS) processes can be applied to encapsulate the active substance by simultaneous co-
47 precipitation of the core material (active product) and the carrier (coating film), or to
48 encapsulate the previous formed active particles by suspending it in a carrier solution and then
49 precipitating the carrier by SAS (Cocero et al., 2009).

50 Optimal operational conditions of pressure and temperature for separation and
51 precipitation processes, such as the SAS technology, are fundamental and can be achieved by
52 the knowledge of the phase behavior of natural extracts in supercritical fluids.

53 In this context, the aim of present work was to investigate the micronization and
54 encapsulation of the *C. sylvestris* extract and the polymer Pluronic F127 by considering the
55 system phase behavior, using the supercritical anti-solvent (SAS) process. The morphology of
56 particles obtained and an estimation of the particle size were characterized by scanning
57 electronic microscopy (SEM) while the interaction between the polymer and the encapsulated
58 extract was verified by differential scanning calorimetry (DSC).

2. MATERIAL AND METHODS

60 <u>Obtention of *C. sylvestris* extract:</u> The supercritical fluid extraction (SFE) of *C.
61 sylvestris* was accomplished in a dynamic extraction unit previously described by Zetzl et al
62 (2003), with the extraction procedure presented by Michielin et al. (2005). Briefly, the
63 extraction consisted of placing 15 g of dried and milled material inside the column to form the
64 particles fixed bed, followed by the control of temperature, pressure and solvent flow rate.
65 The extraction was performed and the solute collected in amber flasks and weighted in an
66 analytical balance (OHAUS, Model AS200S, NJ, USA). The SFE assays were performed
67 with CO_2 added with ethanol (ETOH) or ethyl acetate (ETOAC) as a co-solvent. The
68 extraction was done at 50 ^{o}C, 300 bar and CO_2 flow rate of 8.3 ± 2 g/min for 3.5 h of
69 extraction and using 5 % (wt/wt) of ethanol or ethyl acetate. The SFE assay was performed
70 with 99.9 % pure carbon dioxide, delivered at pressure up to 60 bar (White Martins, Brazil).
71 The resulting mixture from the SFE was separated by using reduced pressure to evaporate the
72 co-solvents in a rotary evaporator (Fisatom, 802, Brazil). The phase equilibrium data which
73 give directions of ideal operational conditions to be applied in the SAS process was obtained
74 in a previous study (Benelli et al., 2014).

75 <u>Supercritical anti-solvent (SAS) encapsulation:</u> The supercritical encapsulation of
76 *Casearia sylvestris* extract in Pluronic F127 was performed in a SFE unit adapted to the SAS
77 process as described by Mezzomo et al. (2013). The organic solution was composed by *C.
78 sylvestris* extract (1:100, wt/wt) and Pluronic F127 (3:100, wt/wt), both dissolved in ethanol
79 or ethyl acetate, with resulting concentrations of 7.9 mg/mL and 24 mg/mL for the extract and
80 polymer, respectively. Ethanol and ethyl acetate was chosen due to the high solubility of the
81 extract and polymer. The precipitation conditions applied were pressures of 90, 130 and 170
82 bar at temperature of 35 ^{o}C and 110, 140 and 170 bar at temperature of 45 ^{o}C, organic
83 solution flow rate of 1.0 mL/min, and constant CO_2 flow rate of 8.43 L/min. The conditions
84 applied were selected based on preliminary precipitation tests and also on previous results of
85 the group and on the phase behavior of the multicomponent system (*C. sylvestris* extract +
86 ethanol or ethyl acetate + CO_2), studied by Benelli et al. (2014). The pressures values tested
87 remain near and above the mixture critical pressure of the mixture for the temperature of 35

88   and 45 ^{o}C. The CO_2 flow rate was chosen with the aim of promoting an intense mixing
89   between the solution (extract + solvent) and the anti-solvent inside the precipitation cell,
90   performed at a CO^2 mass fraction of 95 % (wt/wt). The precipitation experiments started by
91   fulfilling the precipitator vessel with pure CO_2 and, when the desired operating conditions
92   (temperature, pressure and CO_2 flow rate) were achieved and remained stable, 10 mL of pure
93   organic solvent (ethanol or ethyl acetate) was feed into the chamber until the system reached
94   the equilibrium. After that, 30 mL of organic solution (extract + polymer + organic solvent)
95   was pumped, by HPLC pump, inside the precipitator followed by pure CO_2 pumped inside the
96   cell during 15 minutes in order to guarantee total drying of the particles. The quantity of
97   organic solution used enabled the collection of sufficient amount of precipitated powder for
98   analysis. The precipitation chamber was slowly depressurized to atmospheric pressure and,
99   subsequent to the decompression, the sample of precipitated particles retained in the filter was
100 collected for the particle analysis. All samples were stored at temperatures of -18 ^{o}C and
101 protected from light to avoid the decomposition of the product (Mezzomo et al., 2012).

102 <u>Particle morphology and estimated size:</u> The samples of the powder collected from the
103 precipitator were analyzed by scanning electronic microscopy (SEM) (JSM 6390LV-JEOL,
104 USA). A gold sputter was used to cover the samples with a thin layer of gold to allow the
105 light reflection for particle evaluation. An estimation of the mean particle size was measured
106 by ZEISS Image Analysis Software. This procedure was performed according to recently
107 described by Mezzomo et al. (2012).

108 <u>DSC characterization of resultant particles and pure extract:</u> Thermal analyses of the
109 precipitated samples and the *C. sylvestris* extract were performed by differential scanning
110 calorimetry (DSC) (Jade DSC - Perkin Elmer, USA), analyzed as presented by Benelli et al.
111 (2014) Briefly, the samples were analyzed under nitrogen atmosphere for temperatures
112 between -20 and 200 ^{o}C with a heating rate of 10 ^{o}C/min. DSC analyses were conducted in
113 order to give information about the interaction between the carrier (polymer Pluronic F127)
114 and the encapsulated material (*C. sylvestris* extract), and also to estimate modifications of the
115 composition, crystallinity degree and melting temperature caused by the SAS process.

3. RESULTS AND DISCUSSION

117 The results from the scanning electronic microscopy (SEM) of non-precipitated
118 Pluronic F127 and pure Pluronic F127 precipitated at 140 bar and 45 ^{o}C, using ethanol or
119 ethyl acetate as organic solvent, and constant values of solution concentration and anti-solvent
120 flow rate are presented in Figure 1.

121 The results from the SAS process applied, presented in Figure 1, was able to reduce the
122 particle size of pure Pluronic F127 from 612 ± 162 μm to 546 ± 90 μm and 267 ± 40 μm,
123 using ethanol and ethyl acetate at 140 bar and 45 ^{o}C, respectively. The SEM micrographs
124 indicate that the precipitated particles can be considered shapeless.

125 The SEM results of precipitated particles obtained at 90, 130 and 170 bar at temperature
126 of 35 ^{o}C and 110, 140 and 170 bar at temperature of 45 ^{o}C and constant values of solution
127 concentration and anti-solvent flow rate are presented in Figure 2 and Figure 3, using ethanol
128 and ethyl acetate as organic solvent, respectively. The SEM micrographs indicate that the

precipitated particles can be considered shapeless, and the particles size for the samples produced at all conditions tested were within the micrometric range.

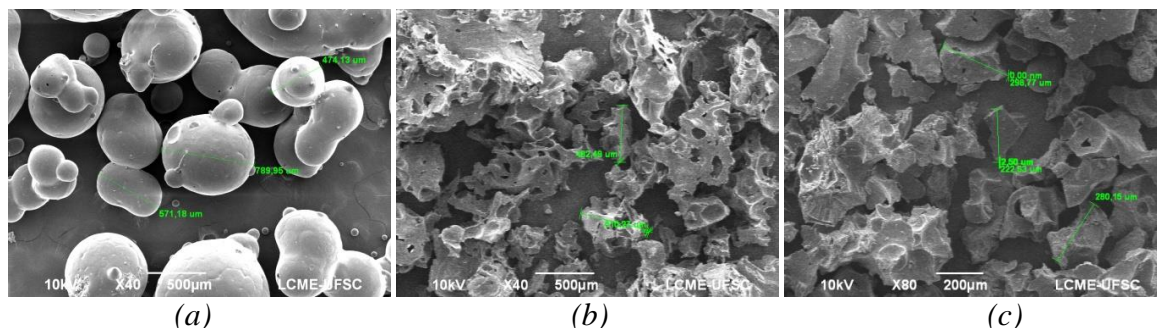*(a)*   *(b)*   *(c)*

Figure 1 - Electronic micrographs obtained by scanning electronic microscopy (SEM) and their respective particle size of pure Pluronic F127 samples of *(a)* non-precipitated (612 ± 162 μm) and precipitated by supercritical anti-solvent (SAS) process at 140 bar ant 45 ^{o}C using *(b)* ethanol as organic solvent (546 ± 90 μm) and *(c)* ethyl acetate as organic solvent at (267 ± 40 μm).

(a)   *(b)*   *(c)*
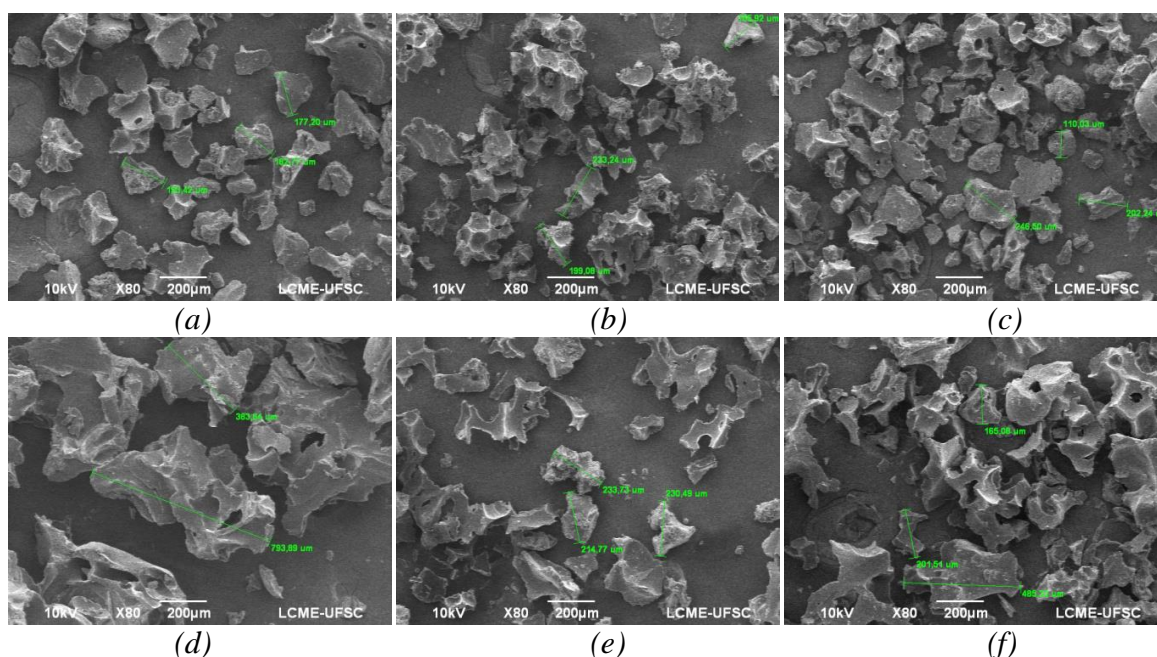
(d)   *(e)*   *(f)*

Figure 2 - Electronic micrographs obtained by scanning electronic microscopy (SEM) of precipitated samples by supercritical anti-solvent (SAS) process and their respective particle size using ethanol as organic solvent: *(a)* 90 bar and 35 ^{o}C (184 ± 8 μm); *(b)* 130 bar and 35 ^{o}C (196 ± 39 μm); *(c)* 170 bar and 35 ^{o}C (186 ± 70 μm); *(d)* 110 bar and 45 ^{o}C (589 ± 290 μm); *(e)* 140 bar and 45 ^{o}C (224 ± 13 μm); *(f)* 170 bar and 45 ^{o}C (183 ± 26 μm).

Considering the results presented in Figures 2 and 3, the temperature effect on the particles aspects was also observed by the particle size results, i.e., larger particles were obtained at the temperature of 45 ^{o}C compared to the ones produced at 35 ^{o}C. Also, the particles obtained using ethanol as organic solvent at 35 ^{o}C (Figure 1) did not present pressure effect on the estimated particle size, instead of 45 ^{o}C, where the increase in pressure reduced the particle size. Analyzing the particles size obtained using ethyl acetate as organic solution, the pressure effect was observed for the temperature of 35 ^{o}C, where the particle size was reduced with the increase in pressure. This behavior was not observed at 45 ^{o}C, indicating that

156 this temperature was not suitable to precipitation process with ethyl acetate because the high
157 particle size produced.
158

(a)   *(b)*   *(c)*
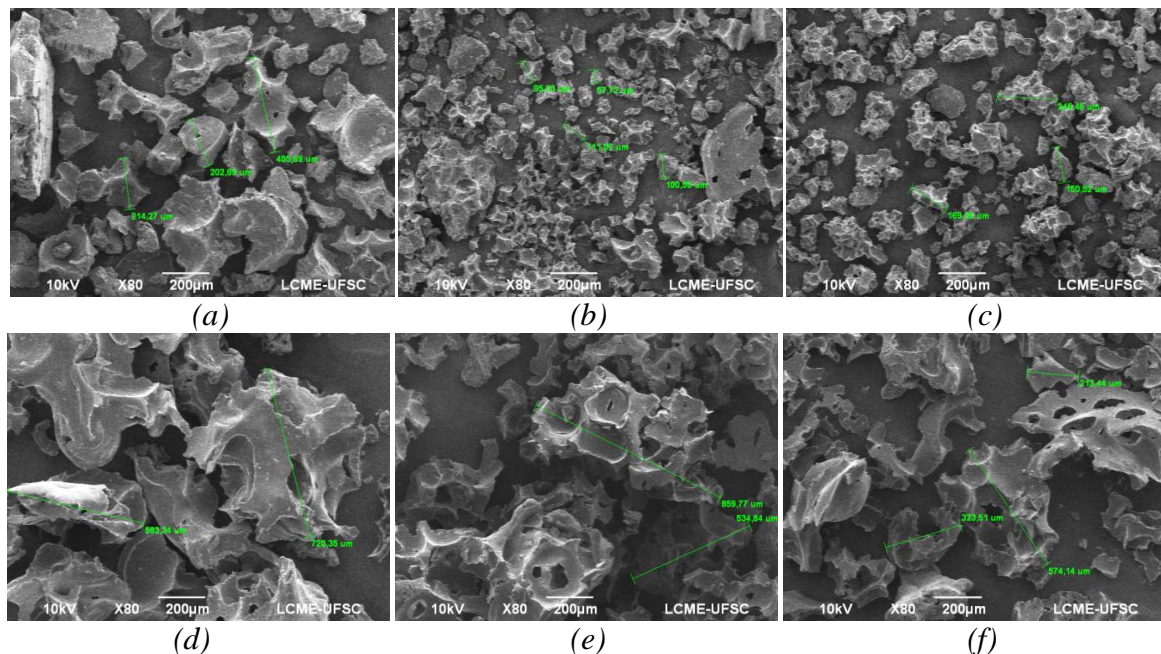

(d)   *(e)*   *(f)*

163 Figure 3 - Electronic micrographs obtained by scanning electronic microscopy (SEM) of precipitated
164 samples by supercritical anti-solvent (SAS) process and their respective particle size using ethyl
165 acetate as organic solvent: *(a)* 90 bar and 35 ^{o}C (274 ± 114 μm); *(b)* 130 bar and 35 ^{o}C (102 ± 8 μm);
166 *(c)* 170 bar and 35 ^{o}C (188 ± 50 μm); *(d)* 110 bar and 45 ^{o}C (652 ± 97 μm); *(e)* 140 bar and 45 ^{o}C (697
167 ± 230 μm); *(f)* 170 bar and 45 ^{o}C (394 ± 255 μm).

168

169   Regarding the particles morphology in Figures 2 and 3, all samples obtained at different
170 pressure conditions and type of organic solvent used (ethanol or ethyl acetate) were shapeless
171 and therefore the pressure effect on particles form was not detected within the range of
172 conditions studied. The same behavior was also reported by Franceschi et al. (2008), in the
173 precipitation of β-carotene and PHBV and co-precipitation from SEDS (Solution-Enhanced
174 Dispersion) process using supercritical CO_2.
175   The DSC results for the SAS samples are observed in Figures 4 and 5, which also
176 presents the heating curves for the pure non-precipitated polymer (Pluronic F127) and for the
177 *C. sylvestris* extract.

178   The DSC heating curves, Figures 4 and 5, showed all SAS samples analyzed. The pure
179 polymer showed one band at near 60 °C, while the *C. sylvestris* extract show no band at the
180 heating curve. The 60 °C peak for the SAS heating curves are probably related to the polymer
181 melting point because the heating curve for the non-precipitated polymer indicate a melting
182 point near 55 ^{o}C (Mezzomo et al., 2012). Regarding the processed samples, the DSC results
183 show a slightly decrease in the fusion/melting temperature (from 60 to near 55 ^{o}C) and also in
184 the enthalpy of fusion, compared to the non-precipitated Pluronic F127. This result may be
185 due to the decrease in the polymer crystallinity with the SAS precipitation or to a partial
186 modification in the crystalline form of the Pluronic F127 during the recrystallization process.
187 Also, the incorporation of the extract inside the polymer (co-precipitation) may be detected by
188 the absence of the crystalline and melting peaks of the active substance, which are normally

189 observed when the active component is not coated by the polymer. Some extracts have no
190 characteristic peak detectable, but only variations on the heat flow in the DSC analysis
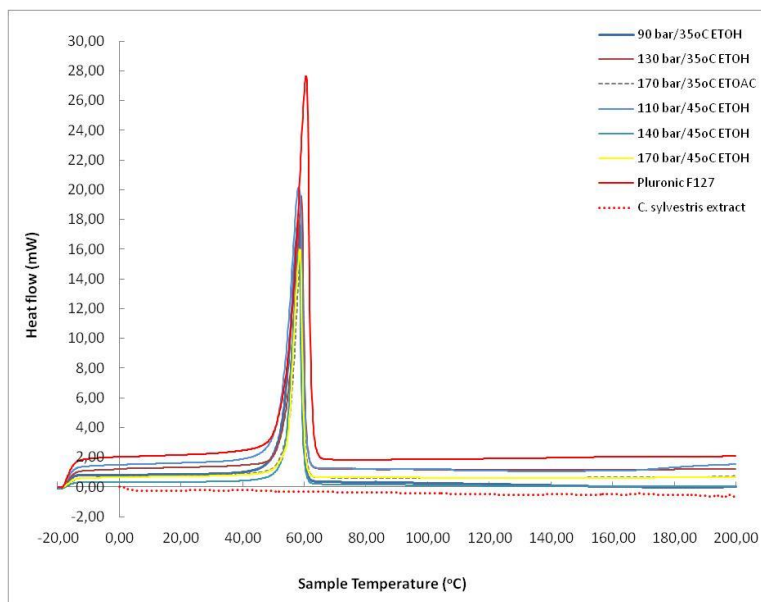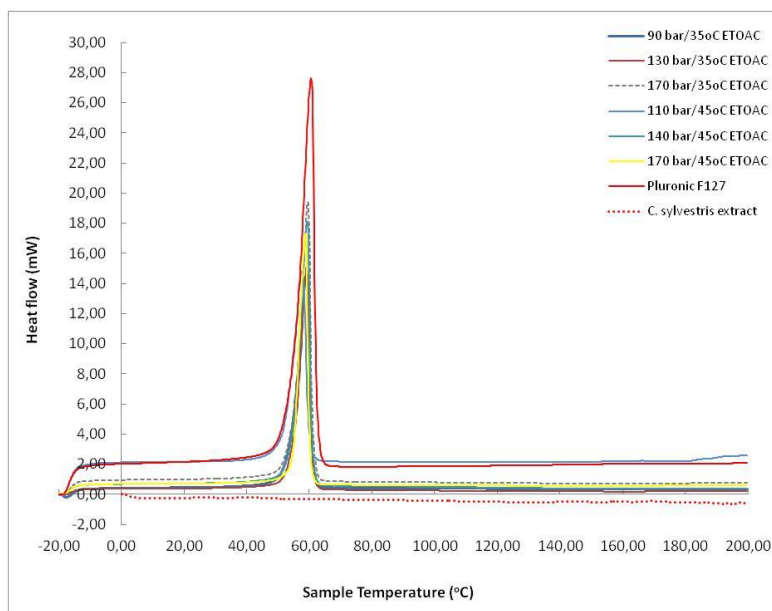191 (Mezzomo et al., 2012; Cocero et al., 2009).

192

193 Figure 4 - Differential scanning calorimetry (DSC) analysis obtained for pure polymer (Pluronic
194 F127), *Casearia sylvestris* extract and precipitated samples obtained by SAS process using ethanol as
195 co-solvent at 35 °C and 45 °C.

196

197 Figure 5 - Differential scanning calorimetry (DSC) analysis obtained for pure polymer (Pluronic
198 F127), *Casearia sylvestris* extract and precipitated samples obtained by SAS process using ethyl
199 acetate as co-solvent at 35 °C and 45 °C.

200 Finally, according to the results for SAS samples and with the absence of heat flow
201 variations - characteristic from *C. sylvestris* extract – (DSC results), it is suggested that

202 encapsulation occurred, i.e., the active substance was incorporated into the carrier matrix
203 (Pluronic F127).

4. CONCLUSIONS

205   SAS process employed to *C. sylvestris* extract was successfully applied to its
206 encapsulation in Pluronic F127, producing micro-particles at all SAS conditions performed.
207 Some operational conditions applied produced particles with smaller size (micrometric order)
208 and better size uniformity, when compared to non-precipitated polymer.

209   Further studies about the co-precipitation of *C. sylvestris* extract and Pluronic F127,
210 including encapsulation efficiency and encapsulation loading are fundamental to define
211 adequate conditions for the particles production by means of supercritical fluid methods.

Acknowledgements

5. REFERENCES

217 Benelli, P.; Rosso-Comim, S. R.; Oliveira, J. V.; Pedrosa, R. C.; Ferreira, S. R. S. Phase
218 equilibrium data of guaçatonga (Casearia sylvestris)extract + ethanol + CO2system and
219 encapsulation using a supercriticalanti-solvent process. *J. Supercrit. Fluids*, 2014,
220 http://dx.doi.org/10.1016/j.supflu.2014.02.007, *In press*.

221 Cocero, M. J.; Martín, Á; Mattea, F.; Varona, S. Encapsulation and co-precipitation processes
222 with supercritical fluids: Fundamentals and applications, *J. Supercrit. Fluids*, v. 47, p. 546-
223 555, 2009.

224 Esteves, I.; Lima, L. M.; Silva, M. L.; Santos, L. S.; Rodrigues, M.; Silva, J. M. S.; Perazzo,
225 F. F.; Carvalho, J. C. T. *Casearia sylvestris* Sw essential oil activity in inflammation in rats
226 induced *Bybothrops alternatus* venom, *Int. J. Pharm. Sci. Ver. Res.*, v. 7(2), p. 28-32, 2011.

227 Ferreira, P. M. P.; Santos, A. G.; Tininis, A. G.; Costa, P. M.; Cavalheiro, A. J.; Bolzani, V.
228 S.; Moraes, M. O.; Costa-Lotufo, L. V.; Montenegro, R. C.; Pessoa, C. Casearin X exhibits
229 cytotoxic effects in leukemia cells triggered by apoptosis, *Chem.-Biol. Interactions*, v. 188, p.
230 497-504, 2010.

231 Franceschi, E.; Kunita, M. H.; Tres, M. V.; Rubira, A. F.; Muniz, E. C.; Corazza, M. L.;
232 Dariva, C.; Ferreira, S. R. S.; Oliveira, J. V. Phase behavior and process parameters effects on
233 the characteristics of precipitated theophylline using carbon dioxide as antisolvent, *J.
234 Supercrit. Fluids*, v. 44, p. 8-20, 2008.

235 Jung, J.; Perrut, M. Particle design using supercritical fluids, J. *Supercrit. Fluids*, v. 20, p.
236 179-219, 2001.

237 Mezzomo, N.; Paz, E.; Maraschin, M.; Martín, Á.; Cocero, M. J.; Ferreira,S. R. S.
238 Supercritical anti-solvent precipitation of carotenoid fraction from pink shrimp residue: Effect

of operational conditions on encapsulation efficiency, *J. Supercritical Fluids*, v. 66, p. 342-349, 2012.

Mezzomo, N.; Ferreira, S. R. S.; Supercritical anti-solvent precipitation of sodium ibuprofen. *In*: I. Mejía, E. Sánchez, C. Pardo, J. A. García (Eds.), *Proceedings of III Iberoamerican Conference on Supercritical Fluids,* 01-05 April, 2013, Cartagena de Indias (Colombia), Applied Thermodynamics and Supercritical Fluids Group, School of Chemical Engineering, Universidad del Valle Cali, 2013.

Michielin, E. M. Z.; Bresciani, l. F. V.; Danielski, l.; Yunes, R. A.; Ferreira, S. R. S. Composition profile of horsetail (*Equisetum giganteum* L.) oleoresin: comparing SFE and organic solvents extraction. *J. of Supercrit. Fluids*, v. 33, p. 131-138, 2005.

Michielin, E. M. Z.; Rosso, S. R.; Franceschi, E.; Borges, G. R.; Corazza, M. L.; Oliveira, J. V.; Ferreira, S. R. S.; High-pressure phase equilibrium data for systems with carbon dioxide, α-humulene and *trans*-caryophyllene, *J. Chem. Thermodyn.*, v. 41, p. 130-137, 2009.

Miguel, F.; Martín, Á.; Mattea, F.; Cocero, M. J. Precipitation of lutein and co-precipitation of lutein and poly-lactic acid with the supercritical anti-solvent process, *Chem. Eng. Process.*, v. 47, p. 1594-1602, 2008.

Oberlies, N. H.; Burgess, J. P.; Navarro, H. A.; Pinos, R. E.; Fairchild, C. R.; Peterson, R. W.; Soejarto, D. D.; Farnsworth, N. R.; Kinghorn, A. D.; Wani, M. C.; Wall, M. E. Novel bioactive clerodane diterpenoids from the leaves and twigs of *Casearia sylvestris*, *J. Nat. Prod.*, v. 65(2), p. 95-99, 2002.

Oliveira, A. M.; Santos, A.G.; Santos, R. A.; Csipak, A. R.; Olivato, C.; Silva, I. C.; Freitas, M. B.; Bassi, C. L.; Cavalheiro, A. J.; Bolzani, V. S.; Silva, D. H. S.; Sakamoto-Hojo, E. T.; Takahashi, C. S.; Soares, C. P. Ethanolic extract of *Casearia sylvestris* and its clerodane diterpen (caseargrewiin F) protect against DNA damage at low concentrations and cause DNA damage at high concentrations in mice's blood cells, *Mutagenesis*, v. 24(6), p. 501-506, 2009.

Reverchon, E.; Della Porta, G.; Falivene, M.G.; Process parameters and morphology in amoxicillin micro and submicro particles generation by supercritical antisolvent precipitation, *J. Supercrit. Fluids*, v. 17, p. 239-48, 2000.

Reverchon, E.; De Marco, I.; Caputo, G.; Della Porta, G. Pilot scale micronization of amoxicillin by supercritical antisolvent precipitation, *J. Supercrit. Fluids*, v. 26, p. 1-7, 2003.

Santos, A. G.; Ferreira, P. M. P.; Júnior, G. M. V.; Perez, C. C.; Tininis, A. G.; Silva, G. H.; Bolzani, V. S.; Costa-Lotufo, L. V.; Pessoa, C.; Cavalheiro, A. J. Casearin X, its degradation product and other clerodane diterpenes from leaves of *Casearia sylvestris*: evaluation of cytotoxicity against normal and tumor human cells, *Chem. Biodivers.*, v. 7, p. 205-215, 2010.

Varona, S.; Kareth, S.; Martín, Á.; Cocero, M. J. Formulation of lavandin essential oil with biopolymers by PGSS for application as biocide in ecological agriculture, *J. Supercrit. Fluids*, v. 54, p. 369-377, 2010.

Zetzl, C.; Lozano, G. A.; Brunner, G. Compilation of batch SFE-Models for natural products. *In*: *I Iberoamerican Conference on Supercritical Fluids* (PROSCIBA). Foz do Iguaçu, Paraná, Caderno de Resumos do PROSCIBA, 2007.